

Stereochemistry of Seven-Coordinate Main Group and d^0 Transition Metal MoleculesZhenyang Lin*[†] and Ian Bytheway[‡]

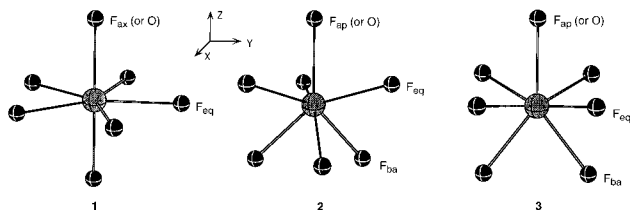
Department of Chemistry, The Hong Kong University of Science and Technology, Kowloon, Clear Water Bay, Hong Kong, and Department of Physical and Theoretical Chemistry, University of Sydney, Sydney, NSW 2006, Australia

Received March 8, 1995[⊗]

Ab initio quantum chemical calculations have been used to study the observed preference for the pentagonal bipyramid (PB) geometry in main group heptafluorides (*e.g.*, TeF_7^- , IF_7 , and XeF_7^+) and main group and transition metal oxofluorides MOF_6^- ($M = \text{I, Re}$) while the capped octahedron (CO) or capped trigonal prism (CTP) geometry is preferred by the analogous transition metal counterparts (*e.g.*, MoF_7^- and WF_7^-). An explanation of these trends is provided by a molecular orbital (MO) model which describes the main group heptafluorides in terms of three non- or antibonding MO's localized largely upon the ligand atoms. These MO's are nonbonding for the PB geometry but slightly antibonding for the CO and CTP geometries because of the lower symmetry of these stereochemistries; thus the PB geometry is predicted for these main group molecules. For transition metal heptafluorides, this MO model predicts that two MO's will not be involved in M–L bond formation as they are localized on the metal atom. Thus for the PB geometry they are nonbonding and slightly antibonding for the CO and CTP geometries. A consequence of the antibonding nature of these orbitals is the slight stabilization of the bonding orbitals and a preference for the CO and CTP geometries. *Ab initio* calculations of MF_7^- ($M = \text{Mo, W}$) molecules predict that the CO and CTP have approximately the same energy and are lower than the PB by approximately 1–4 kcal mol⁻¹. Similar MO arguments may be applied to ReOF_6^- for which the PB geometry was calculated to be lower in energy than the CO and CTP geometries by about 28 kcal mol⁻¹. Total electron densities (ρ) of main group and transition metal fluorides and oxofluorides were compared, and strong ionic character was found in both M–F and M–O bonds. Charge concentration maxima in the core regions of the central atoms were found through analysis of the Laplacian of the charge density ($\nabla^2\rho$) showing that the central atom is distorted by the ligand atoms.

Introduction

An interesting and important aspect of the chemistry of seven-coordination is that three different stereochemistries, the pentagonal bipyramid (PB) (1), the capped octahedron (CO) (2), and the capped trigonal prism (CTP) (3), are observed experi-



mentally.^{1,2} The VSEPR model¹ predicts that, for molecules containing one type of unidentate ligand, the least distance between ligands is maximized in the CO geometry, although not by an amount which results in an energy significantly lower than that of either of the CTP or PB geometry.²

It is convenient to divide heptacoordinate molecules into two broad classes, depending upon the nature of the central atom. When the central atom belongs to the main group, the PB geometry predominates, as observed for TeF_7^- ,^{3,4} IF_7 ,⁵ XeF_7^+ ,³

(RO)₂ TeF_5^- ,⁴ TeOF_6^{2-} ,^{6,7} and $\text{IOF}_6^{8,9}$. A comprehensive overview of the geometries and vibrational spectra of seven-coordinate main group molecules can be found elsewhere.¹⁰ Molecules belonging to the second class, however, adopt all three stereochemistries. For example, ZrF_7^{3-} and HfF_7^{3-} are both pentagonal bipyramidal,¹¹ while MoF_7^- and WF_7^- are capped octahedral,^{12,13} yet NbF_7^{2-} and TaF_7^{2-} are capped trigonal prismatic.^{14,15} The heptacoordinate transition metal oxofluorides MOF_6^{n-} (for example, NbOF_6^{3-} ,¹⁶ TaOF_6^{3-} ,¹⁶ and

* Author to whom all correspondence should be addressed.

[†] The Hong Kong University of Science and Technology.

[‡] University of Sydney.

[⊗] Abstract published in *Advance ACS Abstracts*, January 15, 1996.

- (1) Gillespie, R. J.; Hargittai, I. *The VSEPR Model of Molecular Geometry*; Allyn and Bacon: Boston, MA, 1991.
- (2) (a) Kepert, D. L. *Inorganic Stereochemistry*; Springer Verlag: Berlin, 1982. (b) Kepert, D. L. In *Comprehensive Coordination Chemistry*; Wilkinson, G., Gillard, R. D., McCleverty, J. A., Eds.; Pergamon Press: Oxford, U.K., 1986; Vol. 1, p 31.

- (3) Christe, K. O.; Dixon, D. A.; Sanders, J. C. P.; Schrobilgen, G. J.; Wilson, W. W. *J. Am. Chem. Soc.* **1993**, *115*, 9461.
- (4) Mahjoub, A.-R.; Drews, T.; Seppelt, K. *Angew. Chem., Int. Ed. Engl.* **1992**, *31*, 1036.
- (5) Christe, K. O.; Curtis, E. C.; Dixon, D. A. *J. Am. Chem. Soc.* **1993**, *115*, 1520.
- (6) Christe, K. O.; Sanders, J. C. P.; Schrobilgen, G. J. *J. Chem. Soc., Chem. Commun.* **1991**, 837.
- (7) Christe, K. O.; Dixon, D. A.; Sanders, J. C. P.; Schrobilgen, G. J.; Wilson, W. W. *Inorg. Chem.* **1993**, *32*, 4089.
- (8) Mahjoub, A.-R.; Drews, T.; Seppelt, K. *J. Chem. Soc., Chem. Commun.* **1991**, 840.
- (9) Christe, K. O.; Dixon, D. A.; Mahjoub, A.-R.; Mercier, H. P. A.; Sanders, J. C. P.; Seppelt, K.; Schrobilgen, G. J.; Wilson, W. W. *J. Am. Chem. Soc.* **1993**, *115*, 2696.
- (10) Christe, K. O.; Curtis, E. C.; Dixon, D. A.; Mercier, H. P. A.; Sanders, J. C. P.; Schrobilgen, G. J.; Wilson, W. W. In *Inorganic Fluorine Chemistry: Toward the 21st Century*; Thrasher, J. T., Strauss, H., Eds.; ACS Symposium Series No. 555; American Chemical Society: Washington, DC, 1994; p 66.
- (11) Granzin, J.; Saalfeld, H. Z. *Kristallogr.* **1988**, *183*, 71.
- (12) Giese, S.; Seppelt, K. *J. Fluorine Chem.* **1992**, *58*, 368.
- (13) Giese, S.; Seppelt, K. *Angew. Chem., Int. Ed. Engl.* **1994**, *33*, 461.
- (14) Torardi, C. C.; Brixner, L. H.; Blasse, G. *J. Solid State Chem.* **1987**, *67*, 21.
- (15) Brown, G. M.; Walker, L. A. *Acta Crystallogr.* **1966**, *20*, 220.
- (16) (a) Averdunk, F.; Hoppe, R. *J. Fluorine Chem.* **1989**, *42*, 413. (b) Stomberg, R. *Acta Chem. Scand.* **1983**, *A37*, 412.

ReOF₆⁻¹³) all have pentagonal bipyramidal geometries in which the oxygen atom occupies an axial site.

Initially the relative stabilities of seven-coordinate main group molecules were studied using simple ligand–ligand repulsion calculations. The molecular geometry was idealized by placing each of the seven ligands on the surface of a sphere and the energy of various arrangements (*E*) calculated as a function of the distance separating the ligand pairs (*r*_{ij}) (see eq 1). Thus,

$$E \propto \sum_{i \neq j} \frac{1}{r_{ij}^n} \quad (1)$$

for low values of *n* (0 < *n* < 3) the PB is preferred, for intermediate values (3 < *n* < 6) the CTP is preferred, and for *n* > 6 the CO has the lowest energy.¹⁷ Ligand–ligand repulsion calculations where *n* was kept constant (typically at 6) but where different types of ligand were allowed to move on concentric spheres have also been performed for molecules of the general type MA₆B.² Such calculations reproduced the experimental observations that molecules containing a B ligand with a more repulsive nature prefer the PB stereochemistry with the B ligand in an axial site.

Ab initio calculations of heptacoordinate molecules of the main group have played an important role in the analysis and understanding of experimental data. Calculations of the vibrational frequencies of IF₇ are in excellent agreement with observed values, thus confirming the PB as correct for the ground state geometry.^{5,10} Results of calculations for IOF₆⁻ also helped verify the PB geometry for the ground state of this molecule.^{6,10} Similarly, calculations for the quasi-heptacoordinate molecules XeF₅⁻¹⁸ and XeOF₅^{-19a} were important in establishing their equilibrium geometries. Calculated geometrical parameters and frequencies for the pentagonal planar geometry of XeF₅⁻ are in good agreement with those observed;¹⁸ thus the axial sites of a PB may be thought of as being occupied by sterically active pairs of electrons. Likewise, calculations for XeOF₅⁻ agreed with experiment only when a C_{5v} pentagonal bipyramidal geometry was assumed, in which one axial site is occupied by an oxygen atom and the other by a sterically active lone pair of electrons.^{19a}

A picture of the bonding in these molecules has emerged from *ab initio* calculations. In these PB main group molecules, the bonding between the central and ligand atoms in the equatorial plane can be described in terms of 6-center, 10-electron bonds with some ionic character. Bonding to the axial ligands can be described by the formation of an sp_z hybrid orbital, and the bonds have more covalent character.¹⁰ A molecular orbital (MO) picture which accounts for these findings and which may also be applied to heptacoordinate molecules containing transition metals has, however, not yet appeared. Thus, *ab initio* calculations for seven-coordinate transition metal molecules are presented and an MO model is presented to account for the various experimental findings obtained for these molecules. Additionally, this model is applied to main group molecules and is consistent with that advanced previously.^{3,10}

Theoretical Details

Effective core potentials²⁰ (ecp's) were employed for central atoms in the *ab initio* geometry optimizations. Where the central atom is a main group element, double- ζ ecp basis sets incorporating single- ζ

polarization functions $\zeta_d(\text{Te}) = 0.237$, $\zeta_d(\text{I}) = 0.266$, and $\zeta_d(\text{Xe}) = 0.297$ were used. For the transition metal centers, the outermost core orbitals, which correspond to *ns*²*np*⁶ configurations, were treated explicitly along with the *nd*, (*n* + 1)*s*, and (*n* + 1)*p* valence orbitals.²⁰ The basis sets of the second and third transition series were described by double- ζ representations for the (*n* + 1)*s*/*np*/*nd* electrons, (541/41/31) and (541/41/21), respectively. The Dunning–Huzinaga double- ζ basis set²¹ was used to describe the oxygen and fluorine atoms in all calculations. Geometries were optimized at the restricted Hartree–Fock (HF) level of theory using either the GAMESS-UK²² or Gaussian 92/DFT²³ software package on a Silicon Graphics Indigo2 Extreme work station. Charge density analyses were performed using the theory of atoms in molecules²⁴ as implemented in the AIMPAC²⁵ and MORPHY²⁶ suites of programs.

Results and Discussion

The geometries of the various seven-coordinate molecules presented here were optimized within the framework of three general stereochemistries: the pentagonal bipyramid (1), the capped octahedron (2), and the capped trigonal prism (3). The results of these calculations are listed in Table 1, and where known, experimental values are included for comparison. In all cases, the calculated structural parameters agree quite well with the experimental values: bond lengths and angles are within 0.05 Å and 2°, respectively. In Table 1, we do not include the results of the three structures for IF₇, TeF₇⁻, and XeF₇⁺ because similar results were obtained previously using the Hartree–Fock, MP2, and nonlocal density functional methods.³

No clear preference for one stereochemistry over the others was obtained from the calculations of MoF₇⁻ and WF₇⁻. The CO and CTP isomers of both MoF₇⁻ and WF₇⁻ have similar energies, although the CO is favored in both cases. The PB isomer is higher in energy for both complexes, by approximately 4 kcal mol⁻¹ for the molybdenum complex but only 1.0 kcal mol⁻¹ for the tungsten complex. Because of the very small energy differences between these isomers, frequency calculations were performed for each of these minima (Table 1) and for both complexes the only stereochemistry which yielded no imaginary frequencies was the CO, indicating that this is the correct minimum-energy stereochemistry.

It is also important that the effects of electron correlation in these complexes be studied. Previous calculations of main group MF₇⁻ molecules using Hartree–Fock, Møller–Plesset perturbation, and density functional methods showed that correlation effects are not important for comparing the ordering of the energies of the different isomers.³ For these transition metal complexes we have used configuration interaction (CI) theory to examine the effects of electron correlation and have not performed Møller–Plesset (MP) perturbation calculations, as previous studies have shown that isomer preference in transition metal fluorides is influenced by the level of MP theory used.^{27,28} For example, MP_{*n*} (*n* = 2, 3, or 4) calculations of

(17) Bradford, T. H.; Bartell, L. S. *Inorg. Chem.* **1968**, *7*, 488.

(18) Christe, K. O.; Curtis, E. C.; Dixon, D. A.; Mercier, H. P. A.; Sanders, J. C. P.; Schrobilgen, G. J. *J. Am. Chem. Soc.* **1991**, *113*, 3351.

(19) (a) Christe, K. O.; Dixon, D. A.; Sanders, J. C. P.; Schrobilgen, G. J.; Tsai, S. S.; Wilson, W. W. *Inorg. Chem.* **1995**, *34*, 1868. (b) Ellern, A.; Seppelt, K. *Angew. Chem., Int. Ed. Engl.* **1995**, *34*, 1586.

(20) (a) Hay, P. J.; Wadt, W. R. *J. Chem. Phys.* **1985**, *82*, 270. (b) Hay, P. J.; Wadt, W. R. *J. Chem. Phys.* **1985**, *82*, 299.

(21) Huzinaga, S. *J. Chem. Phys.* **1965**, *42*, 1293. (b) Dunning, T. H., Jr. *J. Chem. Phys.* **1970**, *53*, 2823.

(22) Guest, M. F.; Sherwood, P. GAMESS-UK, Daresbury Laboratory, Warrington WA4 4AD, U.K.

(23) Frisch, M. J.; Trucks, G. W.; Head-Gordon, M.; Gill, P. M. W.; Wong, M. W.; Foresman, J. B.; Johnson, B. G.; Schlegel, H. B.; Robb, M. A.; Replogle, E. S.; Gomperts, R.; Andres, J. L.; Raghavachari, K.; Binkley, J. S.; Gonzalez, C.; Martin, R. L.; Fox, D. J.; Defrees, D. J.; Baker, J.; Stewart, J. P.; Pople, J. A. *Gaussian 92/DFT*, Revision G.1; Gaussian Inc.: Pittsburgh, PA, 1993.

(24) Bader, R. F. W. *Atoms in Molecules: A Quantum Theory*; Oxford University Press, Oxford, U.K., 1990.

(25) Biegler-König, F. W.; Bader, R. F. W.; Tang, T.-H. *J. Comput. Chem.* **1982**, *3*, 317.

(26) (a) Popelier, P. L. A. *Chem. Phys. Lett.* **1994**, *228*, 160. (b) Popelier, P. L. A. *Comput. Phys. Commun.*, submitted for publication.

(27) Marsden, C. J.; Wolyneec, P. P. *Inorg. Chem.* **1991**, *30*, 1681.

Table 1. Calculated and Observed Geometrical Parameters (Å, deg) for Various Seven-Coordinate Molecules, Energies (kcal/mol) Relative to the Lowest Energy Stereochemistry, and Number of Imaginary Frequencies Calculated at the Restricted Hartree–Fock Level

molecule		pentagonal bipyramid (PB) ^a	capped octahedron (CO) ^a	capped trigonal prism (CTP)
MoF ₇ ⁻	Mo–F _{ax} (or Mo–F _{ap})	1.86	1.89 (1.84–1.89)	1.91
	Mo–F _{eq}	1.91	1.88 (1.83–1.85)	1.89
	Mo–F _{ba}		1.90 (1.84–1.90)	1.89
	F _{ap} –Mo–F _{eq}		76.3 (77.5–76.8)	77.8
	F _{ap} –Mo–F _{ba}		131.7 (130.0–132.4)	142.4
	rel energy	4.3	0.0	0.3
	no. of imag freq	2	0	1
WF ₇ ⁻	W–F _{ax} (or W–F _{ap})	1.86	1.90 (1.89)	1.91
	W–F _{eq}	1.91	1.89 (1.86)	1.89
	W–F _{ba}		1.90 (1.91)	1.90
	F _{ap} –W–F _{eq}		75.4 (75.5)	78.6
	F _{ap} –W–F _{ba}		131.0 (131.8)	143.0
	rel energy	1.0	0.0	0.1
	no. of imag freq	2	0	1
IOF ₆ ⁻	I–O	1.78 (1.77)	1.85	1.82
	I–F _{ax}	1.86 (1.82)		
	I–F _{eq}	1.93 (1.88)	1.97	1.93
	I–F _{ba}		1.90	1.95
	O–I–F _{eq}	95.8 (96.5)	80.6	86.8
	O–I–F _{ba}		132.0	145.5
	rel energy	0.0	28.1	29.2
	no. of imag freq	0	2	2
ReOF ₆ ⁻	Re–O	1.65 (1.63–1.67)	1.67	1.68
	Re–F _{ax}	1.91 (1.89–1.93)		
	Re–F _{eq}	1.91 (1.86–1.91)	1.92	1.92
	Re–F _{ba}		1.90	1.91
	O–Re–F _{eq}	93.8 (91.5–95.7)	79.8	83.3
	O–Re–F _{ba}		130.3	142.5
	rel energy	0.0	19.6	31.5
	no. of imag freq	0	2	2

^a Those data in parentheses are available experimental values.^{3–15}

the stability of the octahedral and trigonal prismatic geometries of CrF₆ showed that the former geometry was most stable at the MP2 and MP4DQ levels, while the latter geometry was more stable at the MP3 and coupled cluster levels of theory.²⁷

Single-reference configuration interaction calculations using single- and double-excitation (CISD) energies of the three tungsten structures were performed at their HF-optimized geometries. At this level of theory, the three geometries have almost the same energy. Relative energies in kcal mol⁻¹: CO, 0.0; CTP, 0.02; PB, 0.62. In each calculation the square of the CI coefficient from the HF ground state configuration was approximately 0.84 and those from other configurations were all very small (less than 0.001), indicating that the single-reference treatment afforded by these calculations is valid (*i.e.*, the HF configuration provides an adequate description of the molecule). Further calculations using the method of quadratic CI with single and double excitations (QCISD) gave similar results. Relative energies in kcal mol⁻¹: CO, 0.0; CTP, 0.04; PB, 0.56. On the basis of these results, we conclude that electron correlation effects do not play an important role in the description of the electronic structures of these complexes.

The ReOF₆⁻ molecule, on the other hand, exhibits a significant preference for the PB geometry in which the oxygen ligand occupies an axial site. The energy between the CO and CTP geometries of ReOF₆⁻ is quite large—the CO is lower in energy than the CTP by 11.9 kcal mol⁻¹ and higher than the PB by 19.6 kcal mol⁻¹. Frequency calculations (Table 1) were performed for each of these isomers, and only the PB isomer had no imaginary frequencies.

The small differences in energy between the three geometries for the transition metal heptafluoride complexes are consistent with the sharp singlet observed in the ¹⁹F NMR spectra¹³ and the fact that these different stereochemistries may be found in

the crystal structures of d⁰ transition metal ML₇ systems. The significant preference of ReOF₆⁻ for the PB geometry is in agreement with the observed AB₆ pattern in the ¹⁹F NMR spectrum of this molecule^{9,13} and indicates that the molecule is rigid on the time scale of the NMR experiment.

Molecular Orbital Models

Main Group ML₇ Molecules. Before considering the transition metal heptafluorides, we consider the MO interactions in the analogous main group molecules. An MO diagram for the interactions between the central atom and the ligand σ orbitals is shown in Figure 1. The d orbitals of the main group atom are not shown, as these are much higher in energy than the corresponding s and p orbitals. This assumption is justified by previous calculations which showed that the d-orbital populations in these molecules is small.¹⁰ The left side of Figure 1 shows the orbital interactions for a PB main group ML₇ molecule, while the right side shows the orbital interactions for the CO geometry.

In general, the molecular orbital patterns of both sides of Figure 1 are similar, particularly in four of the M–L bonding MO's. The difference, however, is in the nature of the three nonbonding (or approximately nonbonding) MO's for each geometry: 2a₁' and e₂' for the PB and 3a₁ and 2e for the CO. For the PB geometry, two of these MO's are purely nonbonding (e₂') and are localized exclusively on the ligand centers, while for the CO geometry, the 3a₁ and 2e MO's are slightly antibonding. This slightly antibonding nature is a consequence of the lowered symmetry of the molecule, giving rise to more linear combinations of ligand orbitals possessing the same irreducible representation. For the cases of interest here, the CO (with lower symmetry) has three a₁ and two e combinations but the linear combinations of ligand orbitals for a PB (with higher symmetry) span two a₁', one a₂'', and sets of e₁' and e₂' MO's.

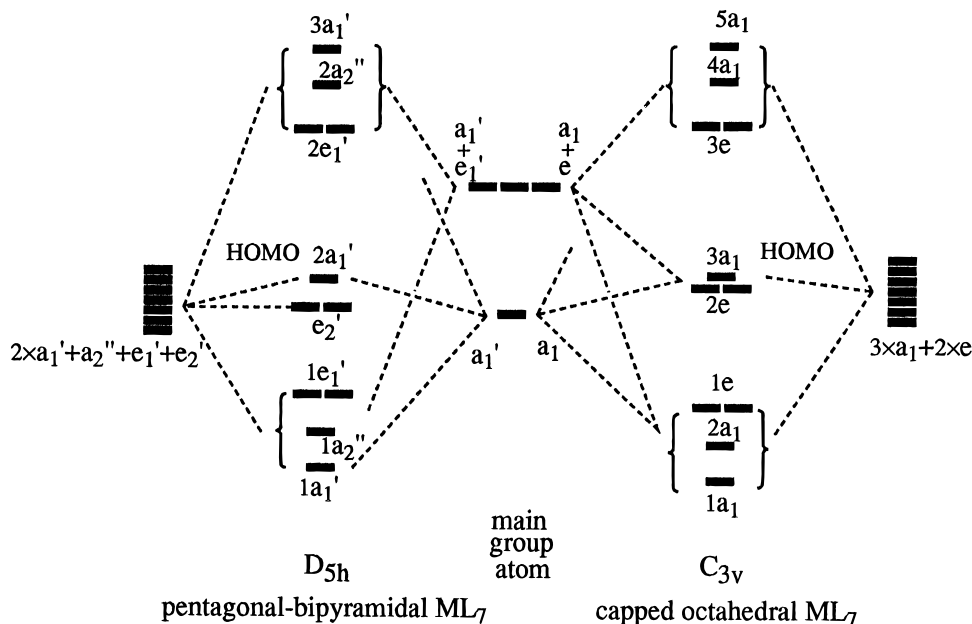


Figure 1. Orbital interaction diagrams for a main group ML_7 molecule. The orbital interactions between the main group and ligand atoms for a PB geometry are shown on the left and for a CO geometry on the right.

The central atom of a main group molecule has only four (s , p_x , p_y , and p_z) orbitals which can interact with the σ orbitals of the ligand atoms. In other words, only four linear combinations of ligand σ orbitals can be stabilized effectively, and consequently, in a seven-coordinate system three linear combinations cannot be stabilized effectively. When these three linear combinations have the same irreducible representations as the four involved in $M-L$ bonding, a destabilization occurs because of orbital mixing of the two sets of MO's. This mixing will, of course, result in the stabilization of the bonding interactions, but the overall effect is one of destabilization.²⁹

In summary, molecules in which a central main group atom is free of valence electrons and has more than four ligands will adopt a geometry with highest symmetry out of the possible alternatives. This idea was noted originally by Giese and Seppelt,¹³ and its electronic origins can now be understood in terms of the MO's of the central atom. This model is consistent with and aids in an understanding of the 6-center, 10-electron bonding description given previously.¹⁰ The preference for various coordination polyhedra, trigonal bipyramid versus square pyramid, octahedron versus trigonal prism, pentagonal bipyramid versus capped octahedron or capped trigonal prism, and square antiprism versus triangular dodecahedron, can be thus explained.

d^0 Transition Metal ML_7 Complexes. A significant difference between the seven-coordinate transition metal complexes and their main group analogues is that the involvement of d orbitals in the $M-L$ bonding is far more significant; thus the orbital interactions described in Figure 1 are not correct for these complexes. An MO diagram showing the interactions between the transition metal d orbitals and the ligand σ orbitals is given in Figure 2. It should be noted that the ordering of the $M-L$ σ orbitals is not necessarily correct but our argument is qualitative in nature and does not require that the orbital orderings be exact.

Figure 2 shows that two nonbonding (or approximately nonbonding) orbitals are localized on the metal atoms, rather than on the ligands. For a PB geometry, two purely d orbitals (e_1'') are nonbonding, while for a CO, the corresponding two MO's are slightly antibonding. Unlike the situation for the main

group molecules discussed above, these MO's are unoccupied in the d^0 transition metal complexes, which means that the greater the destabilization of these two MO's, the greater the stabilization of the $M-L$ bonding MO's. Thus, geometries with lower symmetry are expected to be more stable because these two orbitals are slightly antibonding, and in the case of the PB, these two d orbitals are purely nonbonding and do not help stabilize the $M-L$ bonding MO's at all. Of course, if these two orbitals are occupied (for example, in 18-electron complexes), the PB geometry will be preferred, e.g., $Mo(H)_2(PMe_3)_5$.³⁰ The results of our calculations for MoF_7^- and WF_7^- are in accord with this model (see Table 1).

Earlier calculations^{31,32} have shown that complexes with significant metal(d)-ligand interactions prefer geometries with lower symmetry. Calculations for the three geometries of WH_7^- showed that the CO is 35.7 kcal mol⁻¹ more stable than the PB. The metal-hydride bond length is short, indicating substantial participation of the metal d orbitals in the metal-ligand bonding.^{31,32} The analogous fluoride complexes do not, however, contain such strong metal(d)-fluoride interactions, and the metal(s or p)-fluoride interactions are much more important here. Evidence for this finding is that the metal(d)- $F(p)$ overlap integrals are much smaller than the metal(p)- $F(p)$ overlap integrals, although the energy of the metal d orbitals is usually close to that of the fluorine p orbitals. There is, then, no clear preference for a particular low-symmetry geometry for the d^0 MF_7^- , in agreement with the reported crystal structures.¹⁶

MOF_6^- Molecules. A main group MOF_6^- molecule, such as IOF_6^- , has two extra pairs of electrons localized on the oxygen atom occupying the two π orbitals. As was the case for main group ML_7 molecules discussed above, the main group atom can only stabilize four $M-L$ bonding MO's, leaving five MO's (derived from the linear combination of the ligand orbitals) which cannot be stabilized effectively. A high-symmetry geometry is thus preferred here because the mixing of these five extra "destabilized" orbitals among themselves, or with the $M-L$ bonding orbitals, is minimized. Similarly, the higher symmetry PB stereochemistry for MOF_6^- is also

(29) Albright, T. A.; Burdett, J. K.; Whangbo, M. H. *Orbital Interactions in Chemistry*; John Wiley: New York, 1985.

(30) Lyons, D.; Wilkinson, G.; Thornton-Pett, M.; Hursthouse, M. B. *J. Chem. Soc., Dalton Trans.* **1984**, 695.

(31) Lin, Z.; Hall, M. B. *Organometallics* **1993**, *12*, 19.

(32) Lin, Z.; Hall, M. B. *Organometallics* **1993**, *12*, 4046.

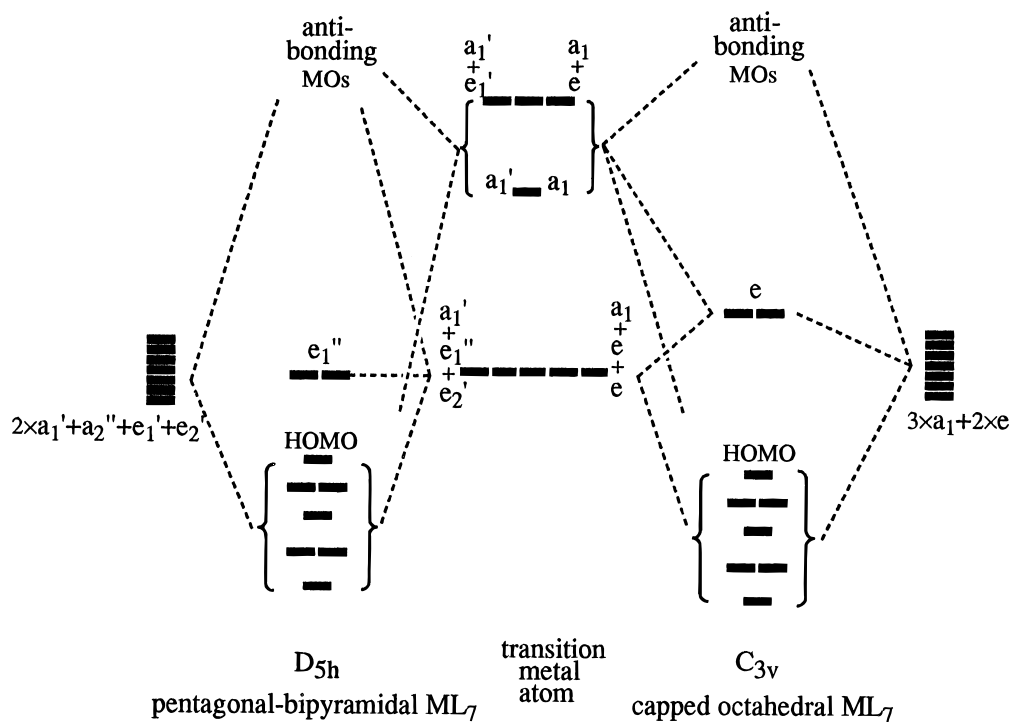


Figure 2. Orbital interaction diagrams for a d^0 transition metal ML_7 molecule. The orbital interactions between the metal and ligand atoms for a PB geometry are shown on the left and for a CO geometry on the right. Note the difference in energy of the lowest unoccupied orbitals of e symmetry in the CO molecule compared to the corresponding e_1'' orbitals in the PB geometry.

Table 2. HOMO–LUMO Gaps Calculated at the Restricted Hartree–Fock Level for Various ML_7 Molecules

	HOMO–LUMO gap (au)						
	XeF ₇ ⁺	IF ₇	TeF ₇ [−]	MoF ₇ [−]	WF ₇ [−]	IOF ₆ [−]	ReOF ₆ [−]
PB structure	0.4496	0.5331	0.5851	0.4696	0.5157	0.4900	0.4987
CO structure	0.4353	0.5237	0.6004	0.4939	0.5475	0.4614	0.4615
CTP structure	0.4360	0.5233	0.5979	0.4896	0.5425	0.4431	0.4162
most stable structure	PB	PB	PB	CO	CO	PB	PB

predicted by the VSEPR model, as the more strongly repulsive oxygen ligand prefers an axial site in the PB and not a capping site in either of the CO or CTP.^{1,2}

The two lone pairs of electrons belonging to the oxygen ligand in transition metal MOF_6^- complexes can be stabilized through interaction with the two nonbonding/slightly antibonding metal d_{xz} and d_{yz} orbitals shown in Figure 2. A PB geometry for the complex results in effective overlap of the metal d_{xz} and d_{yz} with the oxygen p_x and p_y orbitals, and while such overlap occurs in the CO, it will be smaller since the slightly antibonding e orbitals are not pure d_{xz} and d_{yz} , but hybrids corresponding to combinations of d_{xz} and d_{yz} (e') and of d_{xy} and $d_{x^2-y^2}$ (e'') orbitals. In a CTP geometry where the yz plane is defined by F_{ap} and two F_{ba} ligands (see 3), the d_{yz} orbital of the central metal atom is shared by the oxygen and two basal fluorine ligands. From this information, the preference for the different geometries can be deduced as $E(PB) < E(CO) < E(CTP)$ and is supported by our calculations (see Table 1).

These simple MO models explain in a qualitative manner the observed structural preferences in these seven-coordinate molecules and allow for a simple rationalization of experimental results. The MO models proposed here take into account only σ -type interactions and are therefore less sophisticated than corresponding *ab initio* calculations. Correlation between the MO model and *ab initio* calculations can be made by considering the energy separating the highest-occupied and lowest-unoccupied MO's—the largest separation should belong to the most stable isomer. These energies are given in Table 2 and show that this is mostly the case (TeF₇[−] being the only exception), supporting these simple MO models. It should be emphasized

here that these MO models use σ -orbitals only and are not intended to be exact.

Charge Density Analyses

Examination of the total electron density (ρ) and its Laplacian ($\nabla^2\rho$) obtained for these transition metal fluorides and oxo-fluorides was also performed in order to study the effect of the ligand atoms on the charge density at the metal center. Previous studies have shown that the charge density about a metal nucleus is often distorted by the presence of ligands (*i.e.*, it is nonspherical), which may in turn influence the stereochemistry of the molecule.^{33,34} For the sake of comparison, the equilibrium geometries of the heptacoordinate main group molecules IF₇ and IOF₆[−] were also calculated (see ref 35 and Table 1), and for both the PB geometry was calculated to be the most stable stereochemistry, in agreement with previous results.^{3,9}

Initial studies of $\nabla^2\rho$ for IF₇ and MoF₇[−] were performed using the wave functions obtained from the ecp calculations. Despite the explicit inclusion of basis sets to describe the valence space, the calculated atomic graphs (*i.e.*, the number and distribution of critical points in $\nabla^2\rho$ belonging to an atom) contained

- (33) (a) MacDougall, P. J.; Hall, M. B.; Bader, R. F. W.; Cheeseman, J. R. *Can. J. Chem.* **1988**, *67*, 1842. (b) MacDougall, P. J.; Hall, M. B. *Trans. Am. Crystallogr. Assoc.* **1990**, *26*, 101.
 (34) Bytheway, I.; Gillespie, R. J.; Tang, T.-H.; Bader, R. F. W. *Inorg. Chem.* **1995**, *34*, 2407.
 (35) The geometries of IF₇ were optimized using a double- ζ ecp basis set (see Theoretical Details). No imaginary frequencies were found for the PB geometry, while two and one imaginary frequencies were found for the CO and CTP geometries, respectively.

anomalies which suggested that the core electrons are required for a correct description of the valence charge density—as was noted recently in studies of charge densities obtained from semiempirical methods.³⁶ The number of maxima in $-\nabla^2\rho$ (*i.e.*, charge concentration maxima) belonging to iodine was anomalously large (as high as 13 maxima for the CO isomer of IF_7), while results for the molybdenum complexes were similarly at odds with previous all-electron values.³⁷ We conclude from these results that charge density analyses based on the ecp calculations were not useful for these molecules.

The poor description of the total charge density obtained from the ecp calculations is not unexpected, and the problem was overcome by recalculating the total electron density at the ecp-optimized geometries using all-electron basis sets. For both molybdenum and iodine Huzinaga's³⁸ (33333s/333p/33d) basis set was decontracted and supplemented with a polarization function to give a (33333s/3321p/3211d) basis set, and for tungsten Huzinaga's³⁸ (33333s/3333p/333d/3f) basis set was treated similarly to give a (33333s/33321p/33211d/3f) basis set. The properties of the total charge densities were then calculated from wave functions obtained using these all-electron basis sets.

The problem of spurious maxima in $-\nabla^2\rho$ disappeared with the use of these all-electron basis sets, and charge concentration maxima in the cores of the various central M atoms were located. This was a somewhat unexpected result for IF_7 , as core charge concentrations have been previously associated with metal atoms, but not those belonging to the main group. In order to test whether or not these charge concentration maxima were an artifact of the chosen basis set, the total charge density was recalculated for the three isomers of IF_7 using the recently published 6-311G(d) basis set for iodine³⁹ along with the 6-311G(d) basis set for the fluorine atoms. While values of ρ and $\nabla^2\rho$ at the various critical points changed, their number and general arrangement did not, lending strong support to our results.

The location of charge concentration maxima in the various IF_7 molecules will be considered first. Plots of $\nabla^2\rho$ in the axial and equatorial planes of PB IF_7 in the region of the iodine nucleus are shown in Figure 3a,b, respectively. Charge concentration maxima (*i.e.*, (3, -3) critical points in $\nabla^2\rho$) in the iodine core are displaced along the axial bonds, but between the equatorial bonds, which suggests that these charge concentrations (albeit small) are ligand-opposed.^{33,34} The location of charge concentration maxima in the CO isomer is quite different, as shown in Figure 3c. Seven charge concentration maxima in the iodine core were located, arranged in a capped octahedron with the apical maximum located along the I-F_{ap} bond. Thus, the charge concentration maxima are somewhere between being ligand-opposed and being along ligands—a consequence of the symmetry of the molecule because charge concentrations opposed to equatorial fluorine atoms would tend to occur along (or near) a basal I-F bond, and *vice versa*. For the CTP isomer, only six, octahedrally disposed charge concentration maxima were found, which are shown in Figure 3d,e. Five of the six maxima are ligand-opposed and, consequently, are also along I-F bonds (Figure 3d); however, the maxima expected to be opposed to the basal fluorine ligands have coalesced (Figure 3e) and are along the apical I-F bond. Thus of the three

isomers, the most stable is that which minimizes the interactions between ligands, between ligands and core charge concentrations, and also between core charge concentrations themselves.

Different arrangements of core charge concentration maxima were, however, observed for the same three isomers of MoF_7^- . The CO isomer, which has lowest energy, has an arrangement of charge concentration maxima in the molybdenum core which is also in the shape of a capped octahedron. In contrast with the arrangement found for IF_7 though, all of the maxima are ligand-opposed such that no maximum occurs along the Mo-F_{ap} bond, as shown in Figure 4a. Similarly, all of the core charge concentration maxima for the CTP isomer are also ligand-opposed, which can be seen in Figure 4b,c. For the PB isomer, which is the least stable, charge concentration maxima were found along *all* of the Mo-F bonds (Figure 4d,e).

The relationships between fluoride ligands and core charge concentrations are similar to those found previously³⁴ where the bent shape of CaF_2 was explained in terms of the interactions between the fluorine ligand and distortions in the core of the calcium atom; *i.e.*, the most favorable geometry is one which minimizes both ligand-ligand interactions and those between the ligands and core charge concentration maxima in the central atom. This observation appears valid for the range of molecules studied thus far, though a clear understanding of how ligands will distort the core of the central atom is still required. For example, the central atoms of both the PB and CO isomers of IF_7 and MoF_7^- both contain PB and CO arrangements of charge concentration maxima, yet the relationship between the charge concentration maxima and the fluorine ligands depends upon whether the central atom is a main group or a transition metal.

The description of the iodine and molybdenum atoms by ecp's precluded a bonding analysis of the total charge density; thus a bonus of performing the all-electron calculations was that such an analysis was made possible. Using these all-electron wave functions, it was possible to locate bond critical points, construct molecular graphs for each molecule, and calculate charges by integrating over the atomic basins. An interesting result of this analysis, which is demonstrated clearly in Figures 3 and 4, is that bond critical points in all of the complexes occur in regions of charge depletion (*i.e.*, $\nabla^2\rho > 0$), indicative of a predominant ionic bond (or closed-shell interaction²⁴). While this might have been expected for the transition metal complexes, for IF_7 this is an interesting result, as it suggests that the I-F bonding is not covalent (for which $\nabla^2\rho$ would be negative at the bond critical point) as found in the interhalogen molecules ClF_3 ⁴⁰ and ClF_4 ⁴¹

Calculated charges (Table 3) also indicate that the bonding interactions between the central atom and fluorine are predominantly ionic in all of these complexes. Fluorine charges in the various isomers of IF_7 are slightly less negative (approximately -0.6e) than those in the transition metal complexes, (approximately -0.65e) but are still more negative than found in the ClF molecule⁴¹ ($q(\text{F}_{\text{eq}}) \approx -0.3e$ and $q(\text{F}_{\text{ax}}) \approx -0.4$). Nevertheless, these calculated charges do indicate that, for the PB isomer of IF_7 , I-F_{ax} bonding is slightly more covalent than I-F_{eq} bonding, in agreement with the previous MO models¹⁰ and that given here.

For the sake of comparison, calculations of the three isomers of ReOF_6^- , where the oxygen ligand was placed in axial or apical sites, resulted in the PB geometry being most stable over the CO and CTP geometries by 28.1 and 29.2 kcal mol⁻¹, respectively, as expected.

(36) Hô, M.; Schneider, H.; Edgecombe, K. E.; Smith, V. H., Jr. *Int. J. Quant. Chem.: Quantum Chemistry Symposium* **1994**, 28, 215.

(37) Gillespie, R. J.; Bytheway, I.; Tang, T.-H.; Bader, R. F. W. To be submitted for publication.

(38) Huzinaga, S.; Andzelm, J.; Klobukowski, M.; Radzio-Andzelm; Sakai, Y.; Tatewaki, H. In *Gaussian Basis Sets for Molecular Calculations*; Huzinaga, S., Ed.; Elsevier: Amsterdam, 1984.

(39) Glukhovtsev, M. N.; Pross, A.; McGrath, M. P.; Radom, L. *J. Chem. Phys.* **1995**, 103, 1878.

(40) Bader, R. F. W.; MacDougall, P. J.; Lau, C. D. H. *J. Am. Chem. Soc.* **1984**, 106, 1594.

(41) Gillespie, R. J.; Bytheway, I.; DeWitte, R. S.; Bader, R. F. W. *Inorg. Chem.* **1994**, 33, 2115.

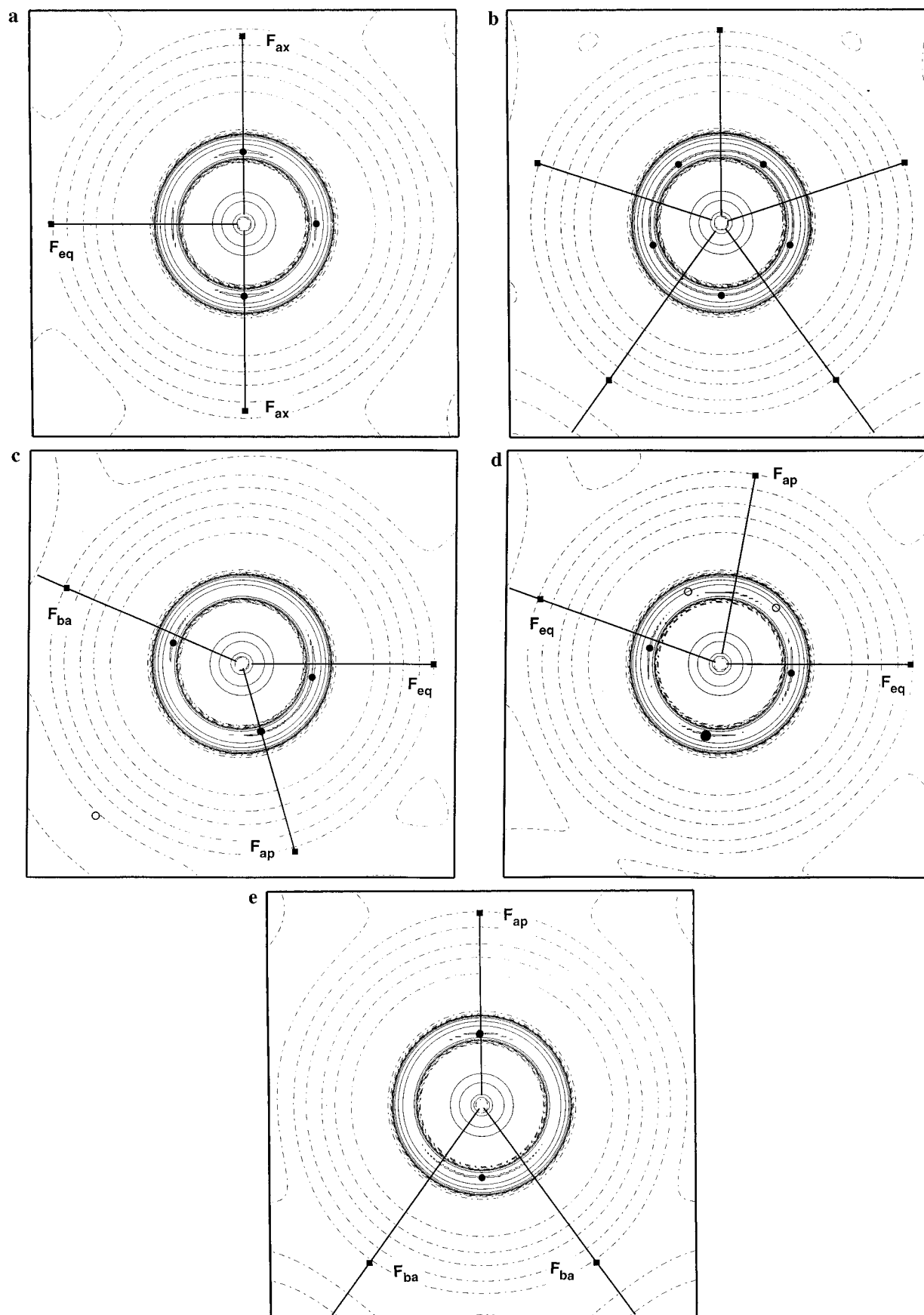


Figure 3. Plots of $\nabla^2\rho$ for the various isomers of IF_7 . Full contours denote regions of charge concentration ($\nabla^2\rho < 0$), and dashed contours denote regions of charge depletion ($\nabla^2\rho > 0$). Bond critical points (*i.e.*, $(3,-1)$ critical points in ρ) between nuclei are denoted by filled squares, and charge concentration maxima (*i.e.*, $(3,-3)$ critical points in $\nabla^2\rho$) are denoted by filled circles. Only critical points in the plotted plane are shown and are labeled according to the ligand to which they belong, and open circles represent the positions of nuclei not projected onto the current plotting plane. (a) The iodine core is shown in the axial plane of the PB geometry. (b) The iodine core is shown in the equatorial plane of the PB geometry. (c) The iodine core for the CO geometry is plotted in the plane containing F_{ap} , F_{eq} , and F_{ba} ligands. (d) The iodine core for the CTP geometry is plotted in the plane containing F_{ap} and two diametrically opposed F_{eq} ligands. (e) The iodine core for the CTP geometry is plotted in the plane containing F_{ap} and both F_{ba} ligands. Note that there is a single charge concentration maximum along the I- F_{ap} bond.

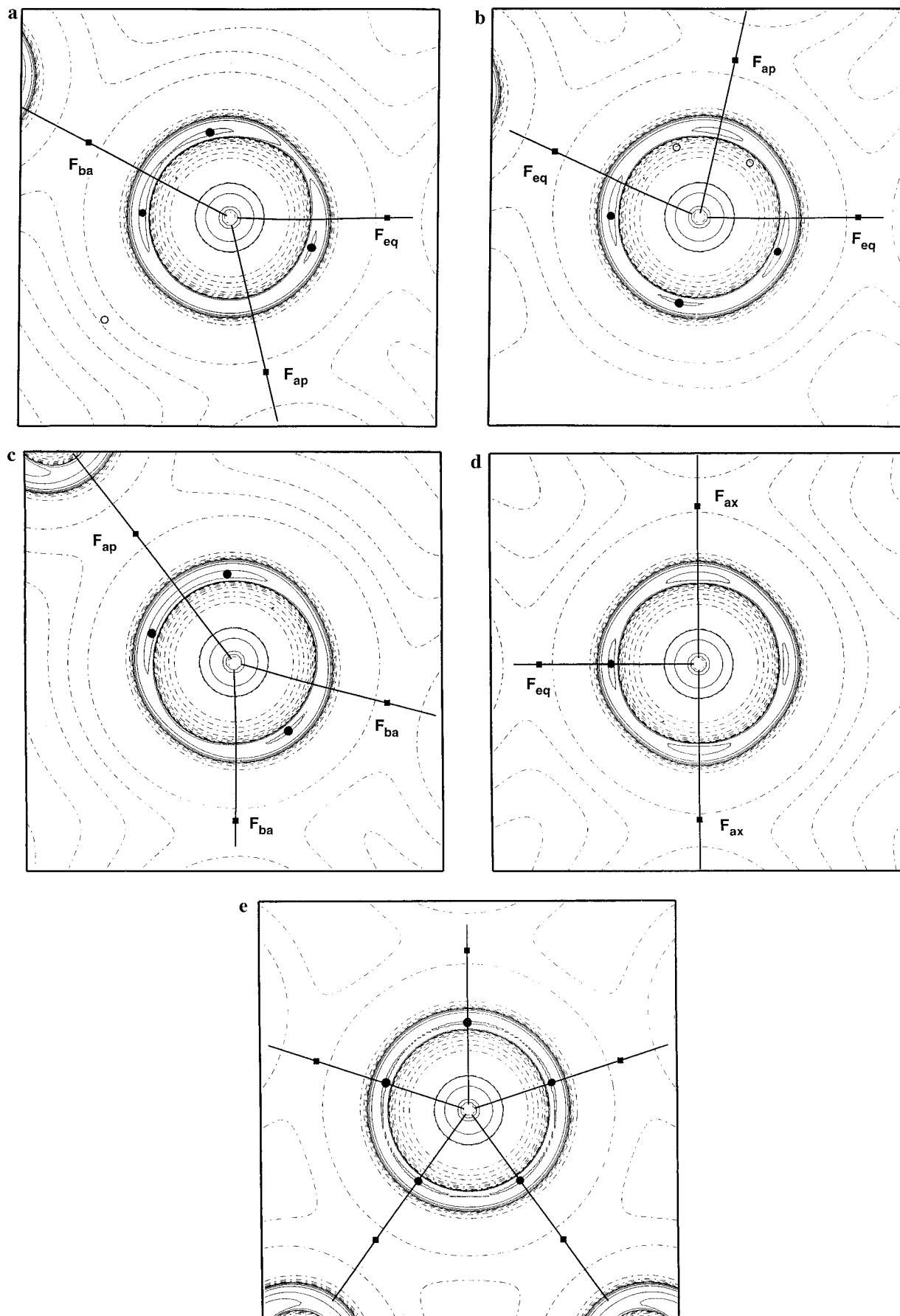


Figure 4. Plots of $\nabla^2\rho$ for the various isomers of MoF_7^- using the same conventions as Figure 3. (a) The molybdenum core for the CO geometry is plotted in the plane containing F_{ap} , F_{eq} , and F_{ba} ligands. (b) The molybdenum core for the CTP geometry is plotted in the plane containing F_{ap} and two diametrically opposed F_{eq} ligands. Note that the charge concentration maxima shown lie slightly out of this plane. (c) The molybdenum core for the CTP geometry is plotted in the plane containing F_{ap} and both F_{ba} ligands. Note that there are now charge concentration maxima opposed to the $\text{Mo}-F_{ba}$ bond. (d) The molybdenum core is shown in the axial plane of the PB geometry. (e) The molybdenum core is shown in the equatorial plane of the PB geometry.

Table 3. Integrated Atomic Charges^a for the MoF₇⁻, WF₇⁻, and IF₇ Molecules

	MoF ₇ ⁻			WF ₇ ⁻			IF ₇		
	PB	CO	CTP	PB	CO	CTP	PB	CO	CTP
<i>q</i> (F _{ax}) or <i>q</i> (F _{ap})	-0.656	-0.644	-0.644	-0.685	-0.679	-0.688	-0.578	-0.605	-0.613
<i>q</i> (F _{eq})	-0.644	-0.641	-0.640	-0.684	-0.679	-0.678	-0.608	-0.591	-0.600
<i>q</i> (F _{ba})		-0.650	-0.649		-0.688	-0.685		-0.604	-0.594
<i>q</i> (M) ^b	3.532	3.517	3.511	3.790	3.780	3.777	4.196	4.188	4.195

^a Populations of the fluorine atoms in each molecule, *N*(F), were obtained by integration of ρ over its atomic basin. The corresponding net charge (in electrons) $q(F) = Z(F) - N(F)$, where $Z(F)$ is the nuclear charge of fluorine. ^b Charges for M (Mo, W, or I) were obtained by subtraction of the integrated charges, *i.e.*, $q(M) = X - \sum q(F)$, where X is the net charge on the molecule and $\sum q(F)$ is the sum of the integrated fluorine charges.

Table 4. Integrated Atomic Charges^a for ReOF₆⁻ and IOF₆⁻

	ReOF ₆ ⁻			IOF ₆ ⁻		
	PB	CO	CTP	PB	CO	CTP
<i>q</i> (O)	-0.625	-0.632	-0.539	-0.946	-0.824	-0.931
<i>q</i> (F _{ax})	-0.717			-0.637		
<i>q</i> (F _{eq})	-0.640	-0.642	-0.625	-0.685	-0.705	-0.650
<i>q</i> (F _{ba})		-0.653	-0.680		-0.650	-0.680
<i>q</i> (M) ^b	3.542	3.517	3.454	4.008	3.889	3.921

^a Populations of the fluorine and oxygen atoms in each molecule, *N*(O or F), were obtained by integration of ρ over its atomic basin. The corresponding net charge (in electrons) $q(O \text{ or } F) = Z(O \text{ or } F) - N(O \text{ or } F)$, where $Z(O \text{ or } F)$ is the nuclear charge of oxygen or fluorine. ^b Charges for the various central atoms were obtained from the other integrated charges in the manner described in Table 3.

Bond critical points and integrated charges were also calculated for these oxofluorides (Table 4), and as was found in the heptafluorides above, the M–F bond is predominantly ionic, rather than covalent, in character. Integrated charges, shown in Table 4, are in accord with this, and fluorine charges are uniformly more negative than was found in the heptafluorides. Interestingly, both Re–O and I–O bond critical points also occur in regions of charge depletion, indicating that these bonds may also be thought of as significantly ionic. Integrated charges indicate that Re–O bonding is more covalent than I–O bonding, as the charge on O in the rhenium complex is about -0.6 compared to about -0.9 in the iodine molecule. This finding is not surprising for the rhenium complex, as a similar situation was found in the V–O bond in VOCl₃³³ and the charge on O is in the range found for other metal oxofluorides.³⁷ For the iodine molecule, this finding is quite different from that for ClOF₃,⁴² in which the Cl–O bond critical point occurs in a region of charge concentration. This difference may be attributed, presumably, to the loss of the iodine valence shell electrons upon formation of the IOF₆⁻ molecule.

The location and number of critical points in $\nabla^2\rho$ in the iodine and rhenium cores are quite different. In IOF₆⁻, the arrangement of core charge concentrations is analogous to that found in IF₇; *i.e.*, maxima were located between (or opposed to) I–F_{eq} bonds and along the I–O and I–F_{ax} bonds. The arrangement of core maxima in ReOF₆⁻ is quite unexpected and consists of a pentagonal antiprism with its pentagonal faces parallel to the plane formed by the F_{eq} atoms. Ring critical points (*i.e.*, (3,+1) critical points in $\nabla^2\rho$) were located along the axial bonds, ruling out the possibility that maxima along these bonds might have been overlooked. This is an interesting and curious result, which may of course be an artifact of the basis set used to describe the rhenium core—in which f electrons are now included and for which relativistic effects (not incorporated in these all-electron calculations) will also be important. These results do show, as in the above calculations, that although the preference for the PB geometry is found for both IOF₆⁻ and ReOF₆⁻, the

distortions of the different central atoms by the ligand atoms are quite different.

Conclusions

Ab initio calculations for various seven-coordinate molecules with different stereochemistries have been performed in order to explain the observations that preferred stereochemistries are dependent upon the type of the central atom. While main group heptafluorides prefer the pentagonal bipyramidal stereochemistry, the analogous transition metal complexes prefer the less symmetrical capped octahedral or capped trigonal prismatic geometries. These observations may be explained using a simple σ -only molecular orbital model:

(i) Main group atoms stabilize only four of the M–L σ -bonding interactions while the remaining three significantly destabilize the overall bonding in either of the CO and CTP geometries. These destabilization effects are somewhat less for the PB geometry, hence the preference for this stereochemistry.

(ii) Transition metal complexes, unlike their main group analogues, have significant d-orbital interactions which affect the preferred stereochemistry. In the less symmetrical CO and CTP geometries, two antibonding d orbitals help to stabilize the M–L bonding orbitals, while in the PB geometry, these d orbitals are purely nonbonding and afford no extra stabilization to the complex. Our findings for these molecules, that the CO and CTP geometries are very close in energy, agree with experimental findings that both may be observed in the solid state. This simple σ -only molecular orbital model is supported by the HOMO–LUMO gaps calculated at the *ab initio* level.

The preference for the PB geometry in both main group and transition metal oxofluorides can also be understood using similar molecular orbital arguments. The high-symmetry PB geometry adopted by main group oxofluorides contains no mixing of the extra ligand orbitals, either among themselves or with bonding MO's, thus favoring this geometry. The interaction between the oxygen ligand and transition metal is also most favorable in the PB geometry, as it does not destabilize the other M–L bonding orbitals. On the other hand, the lower symmetry CO and CTP geometries result in M–O interactions which significantly destabilize the M–F bonding interactions.

Analysis of the total charge densities obtained using ecp's was performed initially; however, the topology of $\nabla^2\rho$ was found to be inadequate even though the valence region of the central atoms was described explicitly. Subsequent all-electron calculations at the ecp-optimized geometries yielded consistent pictures of the charge density and were used instead. The M–L (M = I, Mo, W, Re; L = F, O) bonding was found to be of the "closed-shell" type, indicative of predominant ionic bonding interactions between these atoms.

Distortions of the core regions of the different central atoms were also analyzed through the study of the $\nabla^2\rho$ topology. It was found that the central atoms are indeed distorted by the presence of ligands, in a manner similar to that found in other metal fluorides and oxofluorides.^{33,34,37} For the molecules

having iodine as the central atom, this was an unexpected result, as such distortions of the core have previously been associated with metal atoms only. These charge concentration maxima persisted when calculations using larger, 6-311G(d) basis sets for iodine³⁹ and fluorine were performed. Charge concentration maxima in the heptafluorides were found opposed to M–L ligands in the preferred geometries: the PB for $\overline{\text{IF}}_7$ and the CO or CTP for $\overline{\text{MoF}}_7^-$. Such charge concentration maxima were also found in PB IOF_6^- , but for PB ReOF_6^- , maxima were found above and below the equatorial plane of the molecule arranged in a pentagonal antiprism. Whether or not this topology would persist in the Re core with the use of better

quality basis sets remains to be seen. Nonetheless, these results provide further confirmation of the fact that, upon molecular formation, the charge density of the central atom is indeed distorted and does not remain spherical as is often assumed.

Acknowledgment. Z.L. thanks the Research Council of Hong Kong for financial support. We also thank Professor R. J. Gillespie for his interest and encouragement, Dr. P. L. A. Popelier for a copy of the MORPHY software package, and the reviewers for their useful suggestions.

IC950271O